Engineering Metal Coordination Sites into the Antibody Light Chain

Warren S. Wade, Jong S. Koh, Nianhe Han, Denise M. Hoekstra, and Richard A. Lerner*

Contribution from the Departments of Chemistry and Molecular Biology, The Scripps Research Institute, 10666 North Torrey Pines Rd., La Jolla, California 92037

Received June 18, 1992. Revised Manuscript Received February 5, 1993

Abstract: A three-histidine Zn^{2+} binding site based on the carbonic anhydrase B site has been engineered into the four available sites on the light chain of the fluorescein binding antibody 4–4–20. All mutant antibodies bind fluorescein. Transition metal binding was assayed by tryptophan fluorescence quenching. Two of the four sites exhibit metal affinities consistent with complexation by three ligands. The specificity of the highest affinity site was probed by mutagenesis. For various combinations of histidine, aspartate, and glutamate residues, affinities range from −5 to −10 kcal/mol for Cu^{2+}, −3 to −6.5 kcal/mol for Zn^{2+}, and −3 and −5.5 kcal/mol for Cd^{2+}. Binding is also observed between at least one mutant and Co^{2+} or Ni^{2+}. The second highest affinity site shows a metal-dependent increase in fluorescein binding, indicating a ternary complex. Several ligand combinations give affinities in a potentially useful range for antibody catalysis with only four amino acid changes.

The engineering and production of enzyme catalysts with new specificities is a field of considerable interest with applications in organic synthesis, medicine, and biology. But to produce biological catalysts of new and useful specificity, it is necessary to solve two problems. First, the new enzyme must have some specificity for the substrate of interest. This usually involves a series of low-affinity interactions that cooperatively distinguish between possible substrates. Second, there must be a "catalytic engine", a series of residues and cofactors that are involved carrying out the actual chemistry. This often consists of a small subset of residues that can be readily identified. Natural enzymes tend to be inseparable mixtures of binding and catalysis, especially if the enzyme acts by stabilizing the transition state relative to the ground state.[1] However, in many enzymes, the catalytic activity is mediated by a cofactor with the protein serving as a controlled environment that brings the reaction partners together, matches the reaction requirements, and disfavors side reactions.

It is this class of enzymes that are intriguing targets for protein engineering techniques. Starting with either binding of substrate or cofactor, it should be possible to introduce a binding site for the other. Catalytic antibodies take advantage of the special ability of the immune system to specifically recognize a large variety of potential substrates, and thus the choice of a cofactor becomes the key to activity. A versatile class of enzyme cofactors are the transition metal ions, which are involved in a variety of transformations including DNA and protein hydrolysis, redox reactions, and hydration. Unique to metal ions are their small size and readily tunable properties, where ligand or metal substitution can alter the specificity or the course of the catalyzed reaction. In addition, because ligand geometry can be readily distorted, metal ion catalysis may permit a wider range of catalytic geometries. The facts that useful affinities ($>10^5$) can be achieved using only two or three amino acid residues and that first row transition metal binding tends to stabilize protein structures[2] bode well for the use of metal ions to expand the range of reactions performed by catalytic antibodies. Indeed, two recent reports have shown that antibodies to metal ligand complexes can bind metal productively to perform redox[3] and hydrolytic4[4] reactions.

We have embarked on a comprehensive study of the metal binding potential of a typical antibody with the goal of eliminating any restriction caused by metal complex binding.[4,5] There is considerable evidence for antibody interactions with metal ions,[6] and some direct evidence for antibody–metal complexes,[7] but with the exception of Hg^{2+}, naked metal ions have not proved to be useful antigens.[8] Thus, a more general approach to the production of useful transition metal complexes would be to use genetic engineering techniques to build the coordination complexes into the antibody molecule itself. Because natural antibody–metal interactions tend to segregate with the light chain[7] and because diversity is significantly greater for heavy chain sequences, we have concentrated first on the generation of antibody light chains which coordinate metals. This way our results should be generally applicable to most antibody molecules. Previously, we demonstrated that replacing three residues of an antifluorescein antibody with histidine results in significant cadmium, copper, and zinc binding.[9] Here we report the effects of extensive substitution of the same antibody light chain with potential metal ligands.

The antibody studied is a single chain F_V variant of the high-affinity antifluorescein antibody 4–4–20.[10] The original antibody has been well-characterized by Voss and co-workers.[11] The crystal structure of the Fab complex[12] shows that fluorescein binds in a deep groove between the heavy and light chains, surrounded by tryptophan and tyrosine residues. One face of the hapten is stacked against W33[13,14] of the heavy chain and the other against

(1) Pauling, L. *Am. Sci.* **1948**, *36*, 51–8.
(2) (a) Ghadiri, M. R.; Choi, C. *J. Am. Chem. Soc.* **1990**, *112*, 1630–2. (b) Handel, T.; DeGrado, W. F. *J. Am. Chem. Soc.* **1990**, *112*, 6710–11. (c) Regan, L.; Clarke, N. D. *Biochemistry* **1990**, *29*, 10878–83.
(3) Cochran, A. G.; Schultz, P. G. *J. Am. Chem. Soc.* **1990**, *112*, 9414–5.
(4) Iverson, B. L.; Lerner, R. A. *Science* **1989**, *243*, 1184–8.
(5) (a) Reardan, D. T.; Meares, C. F.; Goodwin, D. A.; McTigue, M.; David, G. S.; Stone, M. R.; Leung, J. P.; Bartholomew, R. M.; Frincke, J. M. *Nature* **1985**, *316*, 265–8. (b) Dardenne, M.; Savino, W.; Berrih, S.; Bach, J. F. *Proc. Natl. Acad. Sci. USA* **1985**, *82*, 7035–8.
(6) Kowolenko, M.; Mccabe, M. J.; Lawrence, D. A. *Clinical Immunotoxicology*; Raven: New York, 1992; pp 401–419.
(7) Lindgärde, F.; Zettervall, O. *Scan. J. Immunol.* **1974**, *3*, 277–85. (b) Baker, B. L.; Hultquist, D. E. *J. Biol. Chem.* **1978**, *253*, 8444–51.
(8) Wylie, D. E.; Lu, D.; Carlson, L. D.; Carlson, R.; Babacan, K. F.; Schuster, S. M.; Wagner, F. W. *Proc. Natl. Acad. Sci. USA* **1992**, *89*, 4104–8.
(9) Iverson, B. L.; Iverson, S. A.; Roberts, V. A.; Getzoff, E. D.; Tainer, J. A.; Benkovic, S. J.; Lerner, R. A. *Science* **1990**, *249*, 659–62.
(10) Bird, R. E.; Hardman, K. D.; Jacobson, J. W.; Johnson, S.; Kaufman, B. F.; Lee, S.-M.; Lee, T.; Pope, S. H.; Riordan, G. S.; Whitlow, M. *Science* **1988**, *242*, 423–6.
(11) For a review, see: *Fluorescein Hapten: An Immunological Probe*, Voss, E. W., Jr., Ed.; CRC: Boca Raton, FL, 1984.
(12) Herron, J. N.; He, X.-M.; Mason, M. L.; Voss, E. W., Jr.; Edmundson, A. B. *PROTEINS: Struct., Funct., Genet.* **1989**, *5*, 271–80.

0002-7863/93/1515-4449$04.00/0

Figure 1. Potential transition metal binding sites on an antibody light chain. (Left) The 4–4–20/fluorescein complex[12] showing the positions of the wild type residues in the binding cleft. Five of the side chains form specific contacts to the hapten. (Right) Distribution of the binding sites on the inner face of the light chain. Residues replaced by histidine in site 2 are dark blue, in site 3 magenta, and in site 4 red. The others are common to more than one site. The fluorescein molecule is in green.

Y32 of the light chain. The oxyanion of the fluorescein ring system forms hydrogen bonds to R34 and S89 (light chain). As shown by mutagenesis,[15] these residues are responsible for the anomalously high binding constant and the pH independence of binding.

Well-characterized transition metal binding sites in proteins are found on both α helices and β sheets.[16] Computer modeling suggests that four potential chelation sites are available in the β sheet segments of the 4–4–20 light chain as shown in Figure 1.[17] Sites 1, 2, and 3 consist of a HXH sequence on one β strand and a third histidine on an adjacent strand, similar to carbonic anhydrase. Site 1, at the bottom of the fluorescein binding pocket, shows the closest fit between the relevant antibody side chain positions and the positions of the carbonic anhydrase ligands. The site exists in most light chains,[14] but it is more than 4 Å away from the binding site often seen for peptide and protein antigens,[18,19] lessening the chance of producing a catalytically active ternary complex. The three other sites show greater potential for productive complexes with most antigens. Site 2 overlaps with 1 on L1 and L3, but it is closer to the frequently seen peptide binding location. Site 3 is close to the antibody surface at L3, and site 4 is close to the surface at L2. Site 4 is contained in a β turn region and is not well-modeled by carbonic anhydrase. However, the Zn^{2+} binding site of carboxypeptidase A has a HXXH sequence in a β turn.[20] In antibodies, a highly conserved framework tyrosine covers the inside face of L2. Replacement of this tyrosine by the first histidine of site 4 should produce a working three ligand metal binding site.

The first three sites involve the replacement of side chains directly involved in fluorescein binding (Figure 1), so that the possibility of simultaneous complexation of both hapten and metal ion appears unlikely. The available crystal structures imply that this should be less a problem for peptide antigens.[19] Site 4 is greater than 7 Å from the fluorescein position in the crystal structure, and therefore it should not prevent hapten binding.

Results

Mutagenesis. Oligonucleotide-directed mutagenesis was performed on a single stranded phagemid containing the complete 4–4–20 F_V construct by the method of Kunkel.[21] Changes in each CDR are performed separately and combined as needed. Overall, nine of the twelve residues facing the heavy chain are mutated in at least one of the antibodies studied. The mutant phagemids are grown in *E. Coli*, thermally induced, and the protein is isolated as inclusion bodies, refolded, and purified by cation exchange. All proteins are named by the differences from 4–4–20. While all DNA constructs tested produce substantial amounts of the induced 27 kd SCA protein, purified protein yields vary significantly. No active protein is obtained for the site 1 mutants CLHH, HLCC, and MLHH. All antibody preparations produced at least two peaks by ion exchange with identical metal and fluorescein binding activities. For the site 1 carboxylate mutants, two well-resolved bands were observed by both ion exchange and native PAGE.

Fluorescein Binding. Fluorescein–antibody association constants are measured by fluorescein fluorescence quenching by protein[22] for affinities $>10^7$ and tryptophan fluorescence quenching by fluorescein for lower affinities. All proteins except the site 3 mutant gave linear Scatchard plots with intercept values >0.60. The site 3 mutant is also significantly less fluorescent than the other proteins. For the high-affinity mutants, where a true maximum quenching constant (Q_{max}) can be measured, all samples are >60% active (4–4–20 SCA is >90% active). Measured affinities are shown in Tables I and II. The excitation spectrum of bound fluorescein for most mutants is the same as 4–4–20, with a maximum at 505 nm. ELEH and HLEH are the exceptions, with a maximum at 487 nm.

General Metal Binding at Sites 1, 2, and 3. Each mutant has been screened for binding to Cd^{2+}, Co^{2+}, Cu^{2+}, Eu^{3+}, Fe^{2+}, Lu^{3+}, Mn^{2+}, Ni^{2+}, Sm^{3+}, Yb^{3+}, and Zn^{2+} by tryptophan fluorescence quenching, using the wild type protein as an external standard.

(13) Amino acids are referred to by a one-letter code: A, alanine; C, cysteine; D, aspartic acid; E, glutamic acid; F, phenylalanine; G, glycine; H, histidine; I, isoleucine; K, lysine; L, leucine; M, methionine; N, asparagine; P, proline; Q, glutamine; R, arginine; S, serine; T, threonine; V, valine; W, tryptophan; Y, tyrosine.

(14) Residue numbering according to: Kabat, E. A.; Wu, T. T.; Perry, H. M.; Gottesman, K. S.; Foeller, C. *Sequences of Proteins of Immunological Interest*, 5th ed.; US Dept. HHS: Washington, 1991.

(15) Denzin, L. K.; Whitlow, M.; Voss, E. W., Jr. *J. Biol. Chem.* **1991**, *266*, 14095–103.

(16) Anfinsen, C. B.; Edsall, J. T.; Eisenberg, D.; Richards, F. M., Eds. *Adv. Protein Chem.* **1991**, *42*.

(17) Roberts, V. A.; Iverson, B. L.; Iverson, S. A.; Benkovic, S. J.; Lerner, R. A.; Getzoff, E. A.; Tainer, J. A. *Proc. Natl. Acad. Sci. USA* **1990**, *87*, 6654–8.

(18) Davies, D. R.; Padlan, E. A. *Annu. Rev. Biochem.* **1990**, *59*, 439–73.

(19) (a) Rini, J. M.; Schulze-Gahmen, U.; Wilson, I. A. *Science* **1992**, *255*, 959–65. (b) Wilson, I. A.; Rini, J. M.; Fremont, D. H.; Feiser, G. G.; Stura, E. A. *Methods Enzymol.* **1991**, *203*, 153–76. (c) Wilson, I. A.; Stanfield, R. L.; Rini, J. M.; Arevalo, J. H.; Schulze-Gahmen, U.; Fremont, D. H.; Stura, E. A. *CIBA Found. Symp.* **1991**, *159*, 13–39. (d) Stanfield, R. L.; Fieser, T. M.; Lerner, R. A.; Wilson, I. A. *Science* **1990**, *248*, 712–19.

(20) Vallee, B. L.; Galdes, A.; Auld, D. S.; Riordan, J. F. *Zinc Enzymes*; Spiro, T. G., Ed.; Wiley-Interscience: New York, 1983; pp 25–75.

(21) Kunkel, T. A. *Proc. Natl. Acad. Sci. USA* **1985**, *82*, 488–492.

(22) Herron, J. N. *Fluorescein Hapten: An Immunological Probe*; Voss, E. W., Jr., Ed.; CRC: Boca Raton, FL, 1984; pp 49–76.

Table I. Fluorescein and Metal Affinities for Three Histidine Mutants[a]

site	H_1	H_2	H_3	Flr	Cu^{2+}	Zn^{2+}	Cd^{2+}	Co^{2+}
wt[b]				6.8×10^9 (1.2)[c]				
1	34	89	91	4.8×10^6 (0.55)	3.1×10^7 (0.45)	3.8×10^4 (1.1)[d]	4.7×10^2 (0.48)	$<10^2$
2	32	34	91	3.8×10^5 (0.51)	3.5×10^5 (0.10)[e]	$<10^2$	$<10^2$	$<10^2$
3	89	91	96	2.6×10^5 (0.95)[e]	2.2×10^5 (0.49)	1.3×10^3 (0.37)	$<10^2$	$<10^2$
4	49	50	53	1.8×10^9 (0.19)	4.4×10^6 (1.1)[f]	10^4–10^5[f]	6.3×10^3 (0.46)[f]	$<10^3$

[a] Kabat *et al* numbering. [b] 4–4–20 SCA. [c] Standard deviation. [d] Two experiments only. [e] Nonlinear scatchard plots. [f] Measured in the presence of fluorescein.

Table II. Fluorescein and Metal Affinities for Varying Ligand Patterns at Site 1

34	36	89	91	Flr	Cu^{2+}	Zn^{2+}	Cd^{2+}	Co^{2+}
H	L	H	H	4.8×10^6 (0.55)[a]	3.1×10^7 (0.45)	3.8×10^4 (1.1)[b]	4.7×10^2 (0.48)	$<10^2$
A	L	H	H	1.3×10^5 (0.15)	1.1×10^5 (0.09)	4.9×10^3 (0.85)[d]	1.1×10^4 (0.07)	1.3×10^2 (0.06)[d]
D	L	H	H	1.6×10^5 (0.08)	3.8×10^5 (0.15)	5.4×10^3 (0.23)	$<10^2$	$<10^2$
Y	L	H	H	3.6×10^6 [c]	1.0×10^6 (0.21)	1.9×10^4 (0.09)[d]	$<10^2$	2.4×10^2 (0.23)[d]
E	L	H	H	4.9×10^5 (1.1)	6.3×10^5 (0.40)	7.2×10^4 (1.2)	9.3×10^3 (0.57)	1.9×10^2 (0.85)[d]
H	L	E	H	7.2×10^7 (0.59)	1.2×10^4 (0.33)	5.3×10^2 (0.57)	$<10^2$	$<10^2$
H	L	H	E	4.5×10^4 (2.1)[e]	1×10^4 [e]	2×10^2 [e]	1.3×10^2 (0.12)	$<10^2$
E	L	E	H	8.5×10^6 (1.2)	3.7×10^4 (0.55)	3.3×10^3 (0.41)	$<10^2$	$<10^2$
E	L	H	E	1.2×10^6 (0.07)	1×10^4 [e]	1.7×10^4 (0.21)	1.2×10^3 (0.02)	$<10^2$
H	L	E	E	7.9×10^4 (0.93)	$<10^4$	NA	$<10^2$	$<10^2$
A	L	H	E	4.9×10^5 (0.76)	$<10^4$	5.7×10^2 (0.91)	2.0×10^2 (0.23)	$<10^2$
H	L	H	D	5.2×10^5 (0.99)	9.9×10^3 (0.54)	3.7×10^2 (0.77)	7.3×10^2 (0.92)	$<10^2$

[a] Standard deviation. [b] Two experiments only. [c] One experiment only. [d] Nonlinear scatchard plots. [e] Measurement near the detection limit.

Other metal ions, especially the second and third row transition metals, have proved incompatible with either protein stability or are practically insoluble at pH 6. A binding event must satisfy three criteria: (1) there are significant differences between wild type and mutant quenching, (2) quenching is saturable and can be reversed by adding EDTA, and (3) the derived Scatchard plot is linear.[23] A typical Scatchard plot and log plots derived from the Scatchard data are shown in Figure 2 for the highest-affinity mutants HLHH and ELHH. Two mutants gave slightly convex Scatchard plots with some but not all metals satisfying all other criteria. These probably represent single sites with other complicating factors. We have indeed observed a large change in fluorescence of ALHH on lowering the pH slightly between 6.0, suggesting that this mutant may be affected by local pH changes. Steric interactions are a likely explanation for the nonlinearity of the YLHH mutant results. In both cases, Zn^{2+} completed with the other metals, indicating a single common interaction site. Metal ions compete with fluorescein binding in the HLHH and ELHH mutants, suggesting that the single site observed is in the antigen binding site.

Unlike the other metals tested, Zn^{2+} does not quench tryptophan fluorescence. However, Zn^{2+} does compete with all metal ions that produce reversible quenching, indicating a common binding site for all metals in a given protein. Unexpectedly, for those mutants with carboxylates at site 1, addition of Zn^{2+} results in an increase in fluorescence, ranging from 30% for ELHH and HLEH to 90% for DLHH. Addition of EDTA reduces the fluorescence to its original levels. A comparison of the competition and direct fluorescence enhancement for ELHH is shown in Figure 3A. The fitted association constants are identical within experimental error. Assuming that the fluorescence enhancement is caused by Zn^{2+} binding gives linear Scatchard plots (Figure 3B). For greater accuracy, the affinities in Table II are derived from this direct plot whenever possible.

Association constants determined from the Scatchard plots are shown in Tables I and II. Each measurement is the mean of at least three experiments with the exceptions noted in the table. The individual data points are archived in the supplementary material. Measured affinities do not vary significantly between preparations of the same metalloantibody, even when the fraction of active protein changes. Affinities naturally divide into two regimes. Above 10^4, the ionic strength is essentially constant over the course of an experiment, and affinities generally vary by less than 15% between measurements. For weaker interactions, the ionic strength necessarily increases with metal concentration and the measured affinities vary more. Cu^{2+} begins to quench 4–4–20 at concentrations above 10 μM, so that low Cu^{2+} affinity mutants also show larger standard deviations.

Dissociation kinetics of Cu^{2+} from HLHH is shown in Figure 4. Cu^{2+} dependent quenching in the presence of an excess of Zn^{2+} decreases exponentially with an apparent lifetime of 90 s.[22] Given the binding constants of Table II, $k_{off} = 9 \times 10^{-3}$ s^{-1}.

Metal Binding at Site 4. Like the wild type antibody 4–4–20, the tryptophan fluorescence of this mutant is unaltered by the addition of metal ions. However, the lacking of quenching could be due to the almost 10 Å distance from the putative metal site to the nearest tryptophan residue. Indeed, as shown in Figure 5, addition of Cu^{2+} at micromolar levels to a complex of fluorescein and protein results in a substantial drop in fluorescence that is not observed for 4–4–20 and fluorescein or for fluorescein alone. The difference spectrum corresponds to free fluorescein, and the change is only observed for samples having significant concentrations of both free antibody and free fluorescein. The same effect is observed at higher levels of Cd^{2+}. The decease in fluorescence is inhibited by millimolar levels of Zn^{2+}, but not Co^{2+}, Ni^{2+}, or Mn^{2+}.[24] Correction of the quenching results with an external standard without metal gives a linear Scatchard plot (Figure 6).

Presence of Cu^{2+} or Cd^{2+} in the assay solution results in an increase in fluorescein affinity by a factor of 2 as shown in Figure 7 for Cu^{2+}. The changes in fluorescein affinity occur over the same range of Cu^{2+} concentrations as the Scatchard plot. Binding constants calculated from the Scatchard analysis are shown in Table I. Because the amount of free antibody and fluorescein is necessarily limited, it is not possible to measure the equilibrium constant for Zn^{2+} by competition closer than an order of magnitude.

Effects of Ligand Replacement at Site 1. Each mutant shows a distinct pattern of metal binding. The behavior of HLHH has already been reported[9] and the results obtained more recently are in qualitative agreement. However, optimization of the assay conditions gives a 10-fold higher affinity for Cu^{2+} than has been reported. As shown in the tables, most proteins exhibit measurable affinities for Cu^{2+}, Cd^{2+}, and Zn^{2+}, while only three mutants

(23) (a) Scatchard, G. *Ann. NY Acad. Sci.* **1949**, *51*, 660–72. (b) Nisonoff, A.; Pressman, D. *J. Immunol.* **1958**, *81*, 126–35.

(24) The lanthanide metals could not be used in this assay because they blocked fluorescein binding to 4–4–20.

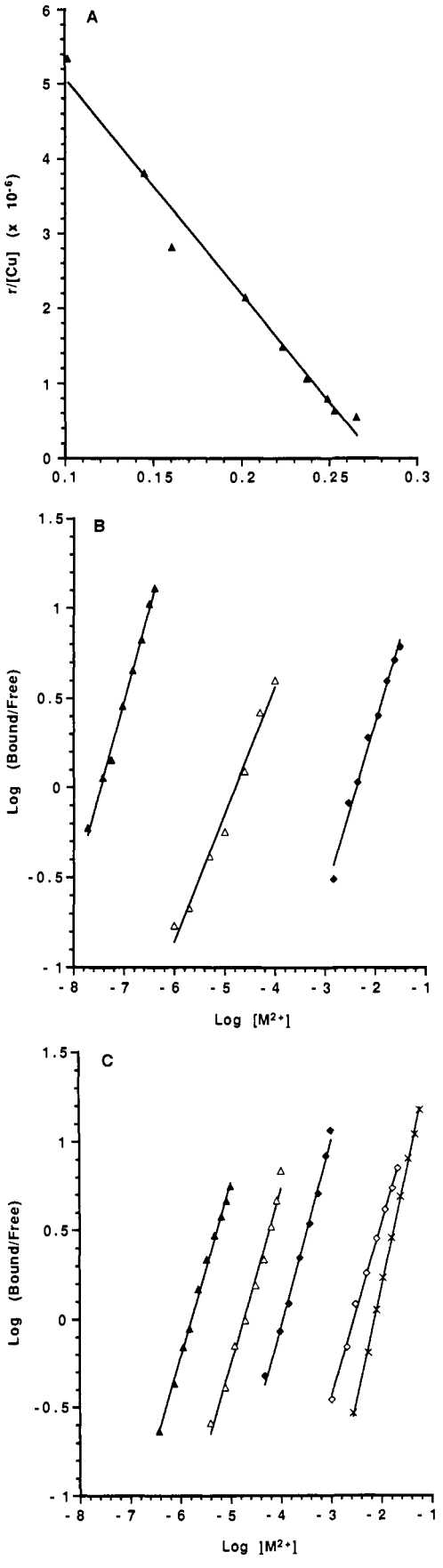

Figure 2. (A) A representative Scatchard plot.[23] r represents the fraction of HLHH fluorescence quenched by Cu^{2+} addition. (B) HLHH Sips plots derived from similar data. The fractions of free antibody are calculated from the Scatchard plots. (C) ELHH Sips plots showing the decrease in ion selectivity following glutamate substitution: (▲) Cu^{2+}, (△) Zn^{2+}, (◆) Cd^{2+}, (◇) Ni^{2+}, (×) Co^{2+}.

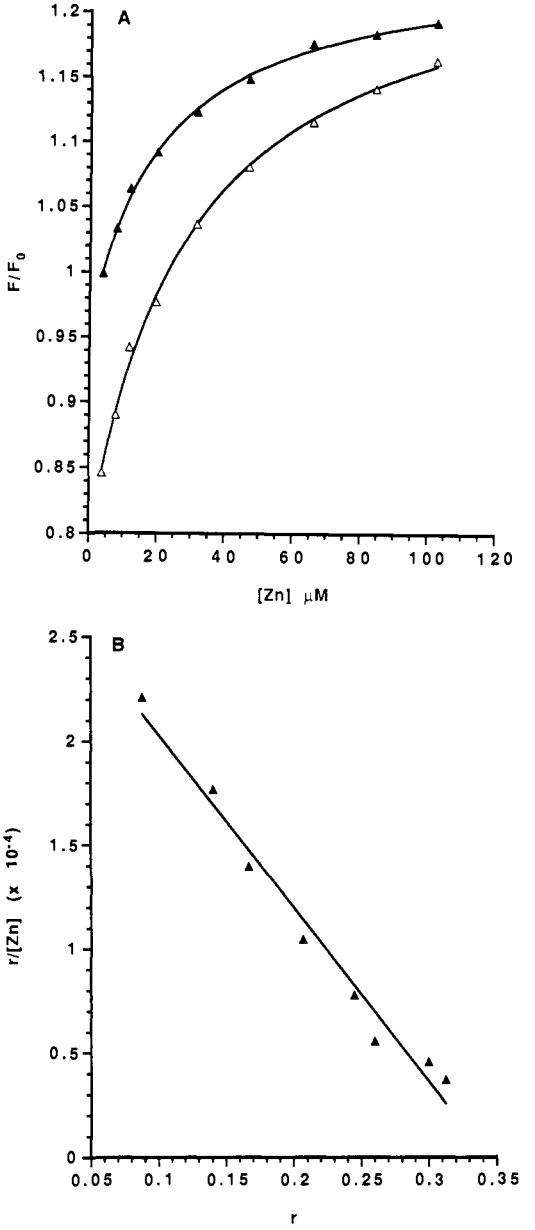

Figure 3. (A) Plot showing the comparison of fluorescence enhancement by Zn^{2+} (▲) and competition between Zn^{2+} and Cd^{2+} (△). F_0 represents the initial fluorescence. The fitted association constants are identical within experimental error. (B) Plot showing the Scatchard analysis of the fluorescence enhancement.

have detectable affinties for Co^{2+}. Titration with Co^{2+} gives significantly convex Scatchard plots. ELHH is the only antibody to exhibit a measurable affinity for Ni^{2+} ($3.4 \times 10^2(0.57)$). The quenching curve meets all three binding criteria. Two mutants, HLHE and ELHE, show specific quenching near the Cu^{2+} measurement threshold. Although the actual affinity is probably less than 10^4 (two other proteins give measurable values of 1×10^4), 1×10^4 represents the upper affinity limit. HLHE shows similar behavior at the Zn measurement threshold.

No quenching attributable to binding is observed for any mutant and Lu^{3+}, Mn^{2+}, or Sm^{3+} and for site 2 or site 3 with any metal except Cu^{2+} or Zn^{2+}. The other three metal ions tested specifically quench one mutant each,[25] but without satisfying the criteria set for a simple binding event. Both Eu^{3+} and Yb^{3+} quench ELHE at concentrations a factor of 10 lower than necessary to quench wild type protein. The Scatchard plot is curved and highly

(25) Addition of Eu^{3+}, Ni^{2+}, Sm^{3+}, and Yb^{3+} produces significant quenching of HLHH at high metal concentrations. However, the dissociation lifetime of >75% of the observed quenching has the same value as Cu^{2+}. By contrast, the lifetime of the Cd^{2+} complex is much shorter.

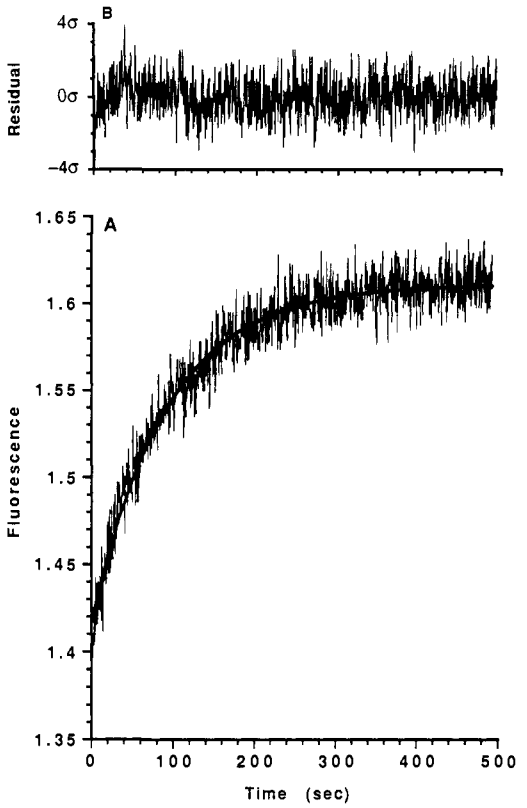

Figure 4. Dissociation kinetics for HLHH + Cu^{2+} in the presence of excess Zn^{2+}, and the standardized residuals for fitting to a single exponential with $t_{1/2}$ = 90 s.

variable. If this represents a binding event, the maximum affinities are 1×10^2 for Eu^{3+} and 3×10^2 for Yb^{3+}. The fluorescence of HLHD is quenched by millimolar levels of Fe^{2+}. Fe^{3+} produces a similar pattern at 10-fold lower concentrations. However, the amount of quenching is linear with added iron and cannot be reversed by EDTA. These observations are most consistent with Fe-mediated oxidation of tryptophan residues.[26]

Discussion

Free energies of complexation derived from Table II are displayed in Table III. As expected, the typical site 1, 2, or 3 mutant binds fluorescein 6–7 kcal/mol less tightly than 4–4–20 (13.4 kcal/mol for SCA with 212 linker[6]), but all mutants show detectable binding. This represents the loss of both the R34 and S91 hydrogen bonds in these mutants, since replacement of just R34 with histidine costs nearly 4 kcal/mol.[11] Mutants containing the E89,H91 pair are anomalously strong binders, possibly because a hydrogen bond exists between fluorescein and the E,H ion pair. Certainly these mutants reconstitute a large part of the R34-mediated affinity. Aromatic residues at position 34 generally show a 2 kcal/mol increase in affinity over other mutants, suggesting there is some stacking against fluorescein. Site 3 quenching is distinctly cooperative, probably because of steric interactions between R34, H89, and H91. As expected from the crystal structure, substitution in L2 has only a small effect upon the site 4 fluorescein affinity. Y49 is strongly conserved in light chain sequences examined to date. The increase in fluorescein affinity upon metal binding to L2 suggests this residue is structurally important to the stability of antibody–antigen complexes.

Evidence for Metal Binding. Although in the absence of a crystal structure the evidence must be considered indirect,[27] all our observations are most consistent with specific complexation of metal ions. First, all reported results represent differences

(26) (a) Uchida, K.; Enomoto, N.; Itakura, K.; Kawakishi, S. *Agric. Biol. Chem.* **1989**, *53*, 3285–92. (b) Uchida, K.; Enomoto, N.; Itakura, K.; Kawakishi, S. *Arch. Biochem. Biophys.* **1990**, *279*, 14–20.

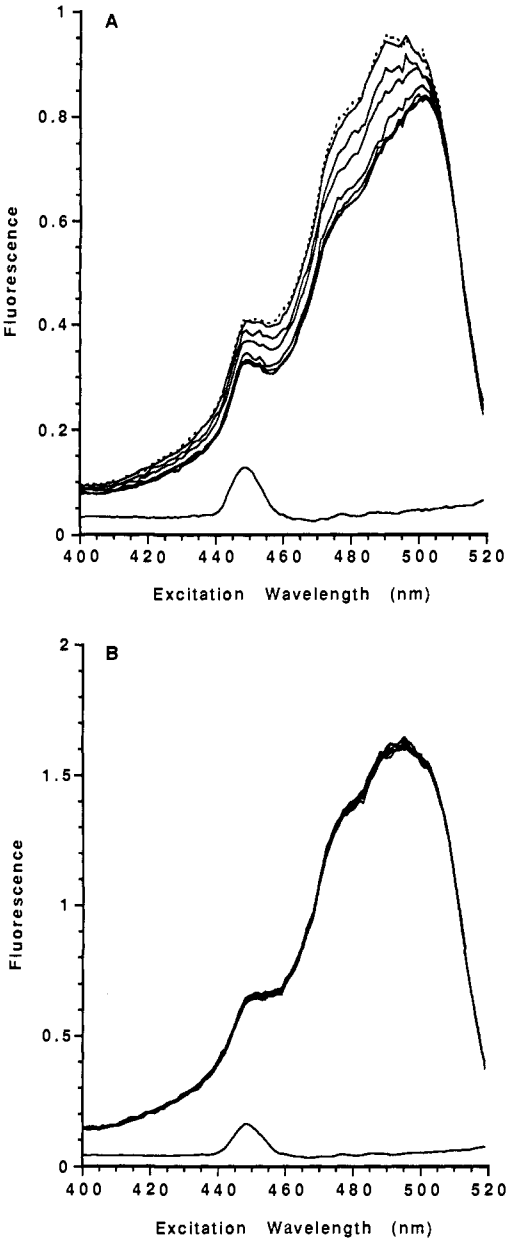

Figure 5. Plot of fluorescein fluorescence quenching with increasing Cu^{2+} concentration: (A) site 4 mutant, (B) 4–4–20 SCA. Solid lines represent excitation spectra corrected for protein loss (<15%). Solid traces proceeding downward represent Cu^{2+} concentrations of 0, 0.10, 0.19, 0.38, 0.66, 1.03, and 1.5 μM and the no fluorescein blank. The dotted trace corresponds to the addition of 1.9 μM EDTA to the final solution.

from 4–4–20. Any change in quenching must be produced by the specific mutations. While we cannot rule out metal-induced partial unfolding or precipitation completely, we consider them unlikely for four reasons. First, Zn^{2+} addition, which often increases protein fluorescence in this system, competes with quenching by other metals. This would require Zn^{2+} to stabilize the antibody structure while all other metals destabilized it. Second, addition of EDTA to a quenched protein solution results in almost complete recovery of the original fluorescence. Third, the dissociation kinetics appear too well-ordered to be a result of other processes. Fourth, the variability and range of metal affinity is quite large, with each site 1 mutant having a unique quenching pattern. It seems unlikely that any mechanism not involving a complex would be so exquisitely sensitive to mutation pattern.

(27) Preliminary time-resolved fluorescence studies indicate a decrease in the fraction of a 3-ns component upon addition of Cu^{2+} to HLHH that is not observed with 4–4–20, consistent with a static quenching mechanism and a true complex. However, the presence of six tryptophan residues in HLHH raises either the required number of exponential terms or the χ^2 value above acceptable limits.

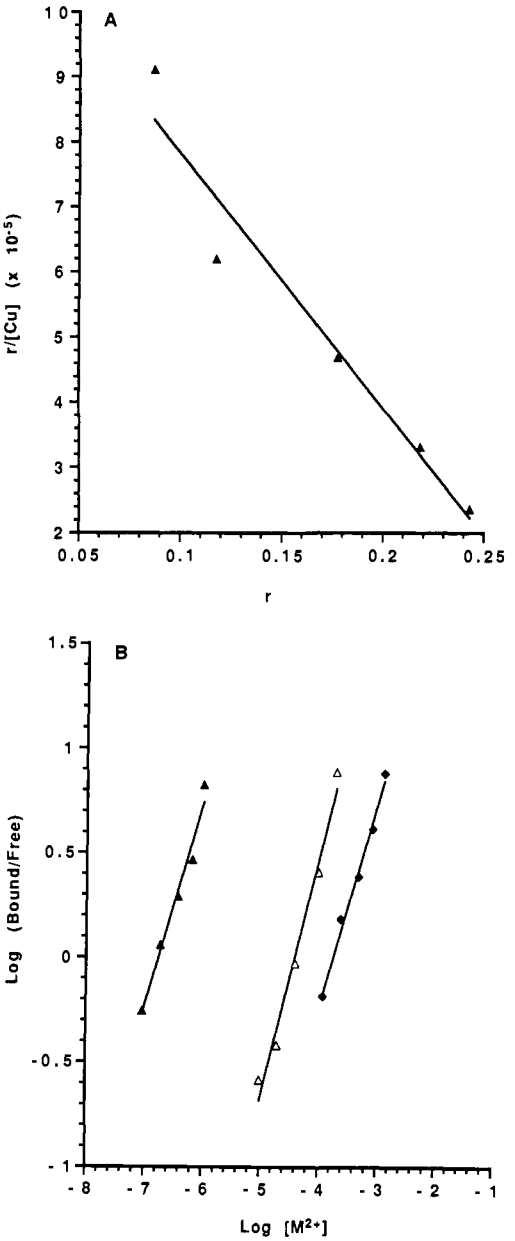

Figure 6. (A) Scatchard plot for Cu^{2+} and site 4. (B) derived Sips plots: (▲) Cu^{2+}, (△) Zn^{2+}, (◆) Cd^{2+}. r represents the fractional decrease of fluorescein fluorescence.

Site 4 binding displays all the characteristics of a ternary complex. Control experiments establish that the enhanced quenching observed is not a direct effect of metal ion on fluorescein or an indirect effect on 4–4–20. The effect is specific for two metal ions at a 1000-fold difference in concentrations. In addition, Zn^{2+} blocks the Cu^{2+}/Cd^{2+} mediated effect, and the effect is reversed on adding EDTA and the Scatchard is linear. The increase in fluorescein binding upon metal addition cannot be explained by charge interactions, since bound Zn^{2+} has no direct effect. A likely explanation is that removal of Y49 decreases the stability of the fluorescein antibody complex by about 1 kcal/mol. Cu^{2+} and Cd^{2+} binding then induces a conformational change that partially reorganizes L2 into the active conformation. The Zn^{2+} complex would then be required to have a different geometry than the Cu^{2+} and Cd^{2+} complexes. Thus this antibody might provide a model for a receptor with distinct but interacting binding sites.

Patterns in Metal Binding. $\Delta\Delta G$'s between histidine and carboxylate mutants, shown in Table IV, reveal that the three ligand positions are not equivalent. Specifically, replacement of either histidine of the HXH sequence gives a mutant that binds Cu^{2+} more than 4.5 kcal/mol less and Zn^{2+} more than 2.5 kcal/mol less. Replacement of H34 by glutamate results in only half that loss. Similar results are seen for a second glutamate substitution. If the second change is at position 34, there is little change in Cu^{2+} binding and a 1 kcal/mol increase in Zn^{2+} binding. When the second substitution is at H89 or H91, Cu^{2+} affinity decreases by 1.5 kcal/mol or more and Zn^{2+} decreases by 1 kcal/mol.

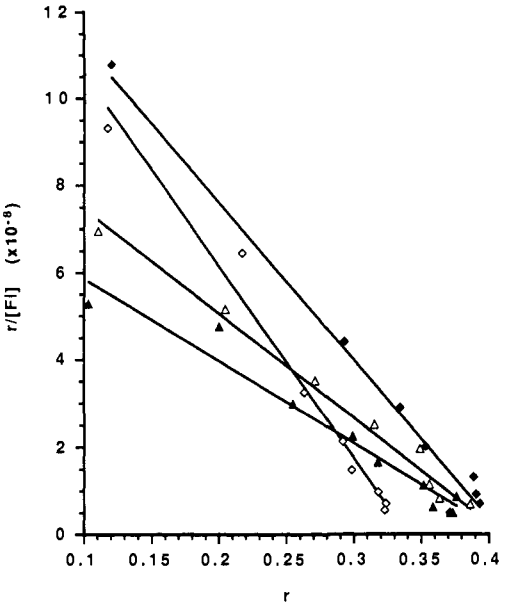

Figure 7. Increased fluorescein binding by the site 4 mutant in the presence of Cu^{2+}: (▲) 0.01, (△) 0.1, (◆) 1.0, and (◇) 12.0 μM Cu^{2+}.

Table III. Free Energies of Complexation Calculated from Table I[a]

34	36	89	91	Flr	Cu^{2+}	Zn^{2+}	Cd^{2+}	Co^{2+}, Ni^{2+}
H	L	H	H	-8.95	-10.05	-6.14	-3.58	
A	L	H	H	-6.83	-6.74	-4.95	-5.44	-2.84
D	L	H	H	-6.96	-7.47	-5.01		
Y	L	H	H	-8.79	-8.06	-5.73		-3.19
E	L	H	H	-7.63	-7.77	-6.51	-5.32	-3.04, -3.40
H	L	E	H	-10.53	-5.46	-3.66		
H	L	H	E	-6.24	-5.36	-3.08	-2.82	
E	L	E	H	-9.29	-6.13	-4.72		
E	L	H	E	-8.13	-5.36	-5.66	-4.13	
A	L	H	E	-7.63		-3.70	-3.10	
H	L	H	D	-7.66	-5.36	-3.44	-3.84	

[a] kcal/mol at 20 °C.

Table IV. $\Delta\Delta G$'s for H to E Substitution[a]

	Cu^{2+}	Zn^{2+}	Cd^{2+}
ELHH-HLHH	2.3	-0.4	-1.8
HLEH-HLHH	4.6	2.5	>0.9
HLHE-HLHH	4.7	3.1	0.8
HLHD-HLHH	4.7	2.7	-0.3
ELEH-HLEH	-0.7	-1.1	
ELHE-HLHE	0.0	-2.6	-1.3
ELEH-ELHH	1.6	1.8	>2.6
ELHE-ELHH	2.4	0.9	1.2

[a] kcal/mol at 20 °C.

Assuming the contribution of A34 is 0.0 kcal/mol, values for the strength of the X34–metal bond are shown in Table V. For Cu^{2+}, the H34 bond is worth one-third the total affinity of HLHH, indicating that this complex is tri-coordinate. The other ligands studied show distinct increases over the A34 antibodies, indicating that they contribute to the complex. For Zn^{2+}, H34 is clearly not optimum, with E34 a better ligand. Cd^{2+} shows a 2 kcal/mol decrease in affinity upon adding H34. The loss is probably caused by steric crowding of the three histidines with the larger Cd^{2+} ion. Affinities of sites 2 and 3 are similar to those of ALHH, suggesting that these complexes are only bicoordinate. Apparently, the protein geometry does not allow three close metal ligand

Table V. $\Delta\Delta G$'s for Ligand Substitutions at Position 34[a]

	Cu^{2+}	Zn^{2+}	Cd^{2+}	Co^{2+}
HLHH–ALHH	−3.3	−1.2	1.9	
ELHH–ALHH	−1.0	−1.6	0.1	−0.2
DLHH–ALHH	−0.7	−0.1		
YLHH–ALHH	−1.3	−0.8		−0.4
HLHE–ALHE		0.6	0.3	
ELHE–ALHE		−2.0	−1.0	

[a] kcal/mol at 20 °C.

contacts. This is consistent with the original modeling,[17] where histidines at site 1 clearly overlapped best with the carbonic anhydrase ligand geometry. Again, a zero interaction energy for the A34 residue gives a complexation free energy of −7.0 kcal for the HXH sequence and Cu^{2+}. This is roughly equivalent to values observed for HXXH on an α helix[28] extrapolated to the same pH assuming direct proton competition. The complexation energy for Zn^{2+} to HXH is −5.0 kcal/mol.

Site 4 is situated in a β turn like carboxypeptidase A rather than a β sheet like site 1 and carbonic anhydrase. Comparison to site 1 is complicated by the presence of fluorescein in the site 4 experiments. However, fluorescein binding differs by only a factor of 2, and the effect of fluorescein on the metal affinity is expected to be similarly small. As measured, Cu^{2+} binds 10-fold more weakly, Zn^{2+} is unchanged, while Cd^{2+} binds 10-fold more strongly. This is consistent with a more tetrahedral ligand geometry coupled with a less hindered binding site.

Comparison with Carbonic Anhydrase and Carboxypeptidase B. Although the absolute affinities of these antibodies for metals are at least 7 kcal/mol weaker, the relative order for Cu^{2+}, Zn^{2+}, Cd^{2+}, and Co^{2+} is the same as for carbonic anhydrase.[29] This preference remains remarkably consistent between mutants that vary 1000-fold in their highest affinity, suggesting that it represents the natural preference for metal binding to ligands with β sheet structures. Ni^{2+} affinity is anomalously low in the metalloantibodies. However, studies of Ni^{2+}–carbonic anhydrase indicate that the Ni^{2+} coordination sphere is at least pentacoordinate,[30] compared to the distorted tetrahedron indicated for the other ions bound.[31] Because the metal ligands in these antibodies are situated at the heavy chain/light chain interface instead of the wide cleft of carbonic anhydrase, we expect steric interactions with the antibody structure to play a significant role in specificity. Thus, Ni^{2+} binding may require rearrangement of the antibody cleft to accommodate the fifth ligand at a substantial free energy cost.

The overall weaker affinity of these proteins is probably due to a combination of factors. Carbonic anhydrase has an extensive network of secondary interactions that serve to orient the metal binding histidines toward the zinc atom.[31] Interestingly, two of the important contacts are from residues on the β strands of the metal ligands: Q92 at the $i-2$ position hydrogen bonds to H94, and E117 hydrogen bonds and ion pairs to the third histidine at position 119. A glutamate–histidine–Zn^{2+} or aspartate–histidine–Zn^{2+} interaction has been observed in over 30 protein structures of dissimilar enzymes.[32] Our results support the proposal that this interaction is important for binding[33] as well as catalysis.[34] Both of these residues might be simulated in the antibody structure by altering conserved residues, though at the risk of losing fluorescein binding entirely.

In contrast to carbonic anhydrase, carboxypeptidase A binds Cu^{2+}, Zn^{2+}, and Cd^{2+} with similar affinities. A smaller range of affinities is also seen for the ELHH mutant with the same coordination sphere as carboxypeptidase A. While HLHH prefers Cu^{2+} over Zn^{2+} by 4 kcal/mol and Zn^{2+} over Cd^{2+} by 2.5 kcal/mol, ELHH prefers Cu^{2+} over Zn^{2+} by 1.3 kcal/mol and Zn^{2+} over Cd^{2+} by 1.2 kcal/mol. Interestingly, Zn^{2+} affinity remains almost unchanged. Site 4, which contains a more carboxypeptidase-like geometry, also exhibits a smaller affinity range. Thus it is likely that the relative insensitivity to metal ion of carboxypeptidase has more than one cause, a combination of a more permissive protein geometry and the effect of the carboxylate ligand.

In so far as they demonstrate that practically useful coordination complexes can be readily achieved in the antibody–antigen binding cleft, the results presented here lay the groundwork for the production of catalytic metalloantibodies. Indeed, we have recently identified an antibody that requires Zn^{2+} activation to hydrolyze a pyridinecarboxylate ester.[35] The reaction velocity is currently limited by the fact that excess substrate produces a catalytically inactive antibody complex containing no Zn^{2+}. A modest increase in affinity for the metal/substrate complex would substantially increase the catalytic efficiency of this antibody, both by decreasing the inhibition and by lowering the free metal ion concentration, consequently decreasing the rate of the background reaction.

Conclusion

We have demonstrated here that the engineering of metal ion sites into β sheet proteins produces metal cofactor sites relatively easily with properties analogous to natural systems. Only the primary interactions are necessary to produce potentially useful affinities, and these can be introduced into almost any light chain. While our current systems are not very selective between ions, they are no worse than those found naturally. A more difficult hurdle will be increasing affinity so that lower concentrations of free ion are present. This is necessary in order to have any *in vivo* activity, given the submicromolar levels of transition metals in biological systems like plasma.[36] The biggest challenge will be finding systems where the binding of metal and substrate lead to productive complexes for catalysis. Fortunately, antigen–antibody union is a diverse process where binding of different antibodies occurs with a variety of contacts even with the same antigen, thereby offering the opportunity to test a wide variety of constructs for catalysis. The substrate of interest can be expected to play a large role in the choice of a particular coordination site as well as the metal studied.

Along with the work on binding sites in α helices our results also point out a possible explanation for the wide natural usage of isolated metal ions as cofactors. Because altering only three residues of a typical protein structure produces a metal site with a useful affinity, a metal ion cofactor is easily included in a new functional enzyme. Evolution can then rapidly improve metal affinity by generating a secondary interaction network that stabilizes the primary metal sphere. This process would make a metal site a relatively common target of convergent evolution, and it suggests that there should be less sequence conservation between metalloenzymes than between enzymes requiring other cofactors. This does indeed appear to be the case.[16]

Finally, the metalloantibodies we have produced so far have shown themselves to be good models for the binding sites of

(28) (a) Suh, S. S.; Haymore, B. L.; Arnold, F. H. *Protein Eng.* **1991**, *4*, 301–5. (b) Todd, R. J.; Van Dam, M. E.; Casimiro, D.; Haymore, B. L.; Arnold, F. H. *PROTEINS: Struct. Funct. Genet.* **1991**, *10*, 156–61. (c) Umaña, P.; Kellis, J. T., Jr.; Arnold, F. H. *ACS Symp.*, in press.

(29) Lindskog, S.; Nyman, P. O. *Biochim. Biophys. Acta* **1964**, *85*, 462–74.

(30) (a) Bertini, I.; Borghi, E.; Luchinat, C.; Monnanni, R. *Inorg. Chim. Acta* **1982**, *67*, 99–102. (b) Bertini, I.; Borghi, E.; Luchinat, C. *Bioinorg. Chem.* **1978**, *9*, 495–504.

(31) Lindskog, S. *Zinc Enzymes*; Spiro, T. G., Ed.; Wiley-Interscience: New York, 1983; pp 77–121.

(32) Argos, P.; Garavito, R. M.; Eventhoff, W.; Rossman, M. G.; Brändén, C. I. *J. Mol. Biol.* **1978**, *126*, 141–58. Valee, B. L.; Auld, D. S. *Proc. Natl. Acad. Sci. USA* **1990**, *87*, 220–4. Christianson, D. W.; Alexander, R. S. *J. Am. Chem. Soc.* **1989**, *111*, 6412–9.

(33) Yamashita, M. M.; Wesson, L.; Eisenman, G.; Eisenberg, D. *Proc. Natl. Acad. Sci. USA* **1990**, *87*, 5648–52.

(34) Krauss, M.; Garmer, D. J. *J. Am. Chem. Soc.* **1991**, *113*, 6426–35.

(35) Wade, W. S.; Jaranghiri, G. K.; Ashley, J. A.; Janda, K. D.; Lerner, R. A. *J. Am. Chem. Soc.*, submitted for publication.

(36) (a) Hay, R. W. *Bio-inorganic Chemistry*; Halsted: New York, 1984. (b) Walter, R. M., Jr.; Uriu-Hare, J. Y.; Olin, K. L.; Oster, M. H.; Anawalt, B. D.; Critchfield, J. W.; Keen, C. L. *Diabetes Care* **1991**, *14*, 1050–6.

metalloenzymes, with the advantage that a new mutant requires only 2–3 weeks to produce. And because antibodies are designed to tolerate large changes in their variable regions, there is a very good chance that any observable difference is the direct result of the changes made and not just a difference in folding or stability. Antibodies also have an independent test for proper folding through their ability to bind the antigen. We consider these properties to be useful in the thorough characterization of metal binding, and we are currently engaged in applying other biophysical techniques to the study of these metal–antibody complexes.

Experimental Section

Materials. Metal ions were purchased as the highest purity chloride salt available from Aldrich Chemical Co., except Fe, which was the mixed ammonium sulfate salt. Solutions were prepared using Milli-Q water and adjusted to pH 6 with potassium hydroxide. Concentrations were calibrated by complexometric titration.[37] Fluorescein solutions were prepared in Milli-Q water and calibrated by UV, using $\epsilon_{495,pH8} = 80\,000$. Metal-free MES buffer was prepared by Chelex treatment of molecular biology grade MES from Sigma. Plasmids pGX8771 and pGX8772 containing the single chain version of 4–4–20 were a gift from Genex.

Oligonucleotide-Directed Mutagenesis. Mutagenesis was performed by the method of Kunkel.[21] Because the expression of 4–4–20 SCA is lethal, the phagemid pGX8771 lacking a promoter was used to prepare the U-containing single stranded DNA template. Changes in each CDR were performed separately, and combined as needed using the *Pst I* site between L1 and L2. The *Cla I*/*Hind III* fragment containing the intact light chain was transferred into the expression phagemid (pGX8772) containing the 212 linker and heavy chain and transformed into *E. coli* strain GX6712 which expresses a temperature sensitive λ repressor.

Protein Expression and Purification. A 400-mL culture of GX6712 containing an expression phagemid was grown at 30 °C to an A600 value of 4–6. The temperature was raised to 42 °C within 5 min and incubated for 1 h. The cells were harvested and lysed in TE (50 mM tris, 1 mM disodium EDTA, pH 8) containing 0.1 mM PMSF using a french press, and the pellet was collected and washed three times with TE/PMSF. The pellet was resuspended in 4 mL of 4 M guanidinium hydrochloride in TKC buffer (50 mM Tris, 50 mM potassium chloride, 10 mM calcium chloride, 0.1 mM PMSF, pH 8) and then centrifuged. The supernatant was diluted into 2 L of TKC and allowed to stand 18 h at 4 °C. The solution was reconcentrated by ultrafiltration (Amicon, 10K membrane) to 120 mL and dialyzed thoroughly against 10 mM MES, pH 6. The dialysate was centrifuged, filtered through 0.22 μm, and applied to a cation exchange column (Pharmacia, mono S). Active protein was recovered by elution with a potassium chloride gradient, dialyzed exhaustively against metal-free MES, pH 6, and stored containing 1.5 mg/mL of PEG 8000. Protein concentration was determined by absorbance at 280 nm, using $\epsilon = 50\,000$. A typical preparation yields 1–2.5 mg of antibody at a concentration of 3 μM.

Fluorescence Measurement. Equilibrium binding studies were performed using an SLM Aminco 500C spectrofluorimeter. Lamp output was calibrated daily using the water raman band (323 nm when excited at 292 nm). Tryptophan fluorescence was recorded with the excitation wavelength at 292 nm (2-nm slit) and emission at 345 nm (7.5-nm slit). Fluorescein was recorded with excitation set to 492 nm (2 nm) and emission set to 530 nm (7.5 nm). Excitation spectra and time traces were recorded using the reference PMT to control for variable lamp output.

Equilibrium Metal Binding at Sites 1, 2, and 3. In a typical experiment, antibody was added to a final concentration of 50 nM to 1 mL of a 2 mM metal-free MES, 2.5 mM calcium chloride, 0.5 mg/mL of PEG 8000, pH 6.0 solution. The solution was equilibrated with occasional mixing at 20 °C for 25 min, and aliquots of a metal ion solution were added. After a 5-min equilibration, the fluorescence was read. Usually, 8–10 data points spanning the sensitive range of the binding curve were collected. The fraction of antibody bound was determined by the fluorescence drop at each point corrected for any changes in the 4–4–20 external standard. Association constants were determined by Scatchard analysis. For mutants exhibiting nonlinear plots, metal ion was added until near saturation, and the resultant r vs cation concentration curve was fitted by nonlinear least-squares techniques. An apparent association constant was determined from the half-quench point of the curve. Competitions between Zn^{2+} and other metals were determined by preparing stock antibody and metal solutions and then adding serially diluted Zn^{2+} to give the same final concentrations of all components as above. Unbound fluorescence was measured by adding EDTA to the lowest Zn^{2+} concentration. The resulting hyperbolic curve was fitted by nonlinear least-squares techniques.

Equilibrium Metal Binding at Site 4. Antibody was added to a final concentration of 20 nM to 1 mL of a 2 mM metal-free MES, 2.5 mM calcium chloride, 0.5 mg/mL of PEG 8000, pH 6.0 solution. The solution was incubated with occasional mixing at 20 °C for 15 min, and fluorescein was added to give a 12 nM final concentration. Aliquots of metal ion were then added, and the fluorescence was read after 5 min. Association constants were determined from 6 data points as above, using a site 4 protein/fluorescein external standard to correct for dilution and protein loss. Competition experiments were done in the same manner as the other sites.

Dissociation Kinetics. A 100-μL sample of protein was equilibrated with metal ion at 20 °C. After 5 min, 900 μL of a zinc-containing quenching solution was added and the increase in fluorescence followed at 0.5-s intervals. Final concentrations were 50 nM, metalloantibody, 2 mM metal-free MES, 2.5 mM calcium chloride, 0.5 mg/mL of PEG 8000, and 400 μM Zn. The data points collected were fitted to a single exponential, and the technical rate constant obtained was corrected using the association constants for Zn^{2+} and the competing metal ion.[22]

Acknowledgment. We thank Prof. Brent Iverson for his substantial contributions to this project, the American Cancer Society for a fellowship to W.S.W., and NIH for a fellowship to J.S.K.

Supplementary Material Available: Tables of apparent fraction bound versus metal or fluorescein concentration for all experiments mentioned in the text (19 pages). Ordering information is given on any current masthead page.

(37) Schwarzenbach, G.; Flaschka, H. *Compexometric Titrations*, 2nd Engl., ed.; Methuen: London, 1969.